International Journal of Mechanical, Industrial and Aerospace Sciences
ISSN: 2517-9950
Vol:13, No:8, 2019

Assessment of Ultra-High Cycle Fatigue Behavior of EN-GJL-250 Cast Iron Using Ultrasonic Fatigue Testing Machine

Saeedeh Bakhtiari, Johannes Depessemier, Stijn Hertelé, Wim De Waele

***Abstract*—** High cycle fatigue comprising up to 10^7 load cycles has been the subject of many studies, and the behavior of many materials was recorded adequately in this regime. However, many applications involve larger numbers of load cycles during the lifetime of machine components. In this ultra-high cycle regime, other failure mechanisms play, and the concept of a fatigue endurance limit (assumed for materials such as steel) is often an oversimplification of reality. When machine component design demands a high geometrical complexity, cast iron grades become interesting candidate materials. Grey cast iron is known for its low cost, high compressive strength, and good damping properties. However, the ultra-high cycle fatigue behavior of cast iron is poorly documented. The current work focuses on the ultra-high cycle fatigue behavior of EN-GJL-250 (GG25) grey cast iron. An ultrasonic (20 kHz) fatigue testing system is developed and instrumented for testing at ambient temperature, and hourglass shaped cast iron specimens with circular cross-section are designed to be excited in resonance. The temperature of the specimen is measured using a pyrometer and controlled by ventilating air. The displacement at the free end of the specimen (which is linked to stress at the reduced section) is measured using an accurate laser sensor, whose analysis requires careful test preparation and data analysis. The high resonance frequency allowed to characterize the S-N behavior of the cast iron of interest within a matter of days, and repeat the tests to quantify the natural scatter in fatigue resistance. The obtained results will be used in a research project that aims to optimize the design of machine components with respect to weight and durability.

***Keywords*—**GG25, cast iron, ultra-high cycle fatigue, ultrasonic test.

I. Introduction

CONVENTIONAL fatigue testing machines have a limited loading frequency (often below 200 Hz) which is a restrictive factor for studying fatigue strength in the gigacycle regime [1]. Performing a test up to 10^{10} cycles would take more than a year at 200 Hz. Ultrasonic fatigue testing offers a practical solution, allowing to test specimens in the kilohertz frequency range. This test would take about six days to finish at the frequency of 20 kHz.

By limited testing equipment in the aspect of applied frequency, the conventional, standardized fatigue strength data are limited to roughly 10^7 cycles. However, knowledge about the fatigue resistance of materials up to 10^9 and even 10^{10} cycles is critical in high speed rotating machine components such as diesel engines for ships and high speed trains, turbine engines, and car engines [1].

The conventional design codes such as Eurocode [2], [3] assume a fatigue limit after 5×10^6 cycles for some materials (including steels), while some researchers such as Kikukawa (1965), Ebara (1987), and Murakami (1994) proved failure of metallic structures after 10^7 cycles [1]. Some recent researchers such as Bathias [4] and Sonsino [5] also showed the reduction of fatigue strength at ultra-high cycles of loading.

The fatigue life in low stress amplitude tests is dominated by crack initiation [6]. Crack nucleation can include up to 99% of the fatigue life in most metals so the propagation takes place fast [7].

The origin of crack nucleation is subsurface for low amplitude tests on materials containing internal defects (e.g. inclusions) according to Mughrabi [8], and in case of failures after 10^7 cycles according to Bathias et al. [1]. One reason could be the application of very low stress amplitude which is not adequate for plastic deformation at the surface of the specimen. Consequently, interior defects become the crack initiation site [1]. Another reason, according to [7], is the higher probability of existence of a flaw in the interior of the material.

The stress concentration at the inclusion inside the specimen causes crack initiation which can lead to formation of optically dark area (ODA) around the inclusion [9]. After the ODA is formed, early crack growth occurs resulting in the formation of a fish-eye. Then, the steady crack growth phase takes place, which is followed by the fast crack growth phase and the failure of the specimen [10].

In 1911, Hopkinson developed the first resonant system that operated at 116 Hz. Until then, the highest achievable load frequency with a mechanical system was 33 Hz. Later, in 1950, Mason developed the first ultrasonic fatigue testing machine, capable of transforming an electrical signal into mechanical vibration at 20 kHz [11]. The machine developed by Mason is still the basis of most of the current ultrasonic testing devices [1].

II. Ultrasonic Fatigue Test Procedure Development

We have developed an ultrasonic fatigue testing machine for performing the fatigue tests. A schematic of the testing equipment is illustrated in Fig. 1. This machine is composed of an electric power generator, a piezoelectric convertor

Saeedeh Bakhtiari, Johannes Depessemier, Stijn Hertelé, and Wim De Waele are with the department EEMMeCS, Ghent University, Belgium (e-mail: Saeedeh.bakhtiari@ugent.be, Johannes.Depessemier@UGent.be, Stijn.Hertele@UGent.be, Wim.DeWaele@UGent.be).

(transducer), a booster, and an ultrasonic horn. It is made and calibrated to vibrate at 20 kHz. The specimen should also be designed to have the same vibrational frequency so, it will resonate in free vibration rather than forced vibration as the conventional fatigue testing machines operate [1], [12], [13].

In the process of fatigue testing at kilohertz frequencies, a great amount of heat is generated, which would affect the specimen's fatigue lifetime [13]. According to [7], microstructural transformation in the process of fatigue testing is considered as the main reason for heat generation.

As Wang et al. [7] explains, metals have an elastic macroscopic behavior around 10^9 cycles except around metallurgical defects (inclusion, porosity, super grain), and flaws. According to [6], the cyclic plastic zone formed around the crack causes a great amount of heat dissipation.

Temperature increase causes decrease of the modulus of elasticity and as a result decreases the resonance frequency and increases the displacement amplitude [12], [14]. Therefore, a solution needs to be defined to keep the specimen's temperature within the acceptable range. Different approaches have been proposed to accomplish this goal with their own pros and cons. The first solution is using refrigerants which cool the specimen effectively, but may alter the mechanical properties at the surface of the specimen [13], [15]. The second option is performing and pausing the test in intervals. Another option is using compressed air as a cooling system [16]-[18], which is the method applied in the current project. A combination of the pulse-pause method and compressed air could be used alternatively [14], [19].

In the tests with none or insufficient cooling, the specimen's temperature goes over 120°C in very few seconds; so, the specimen's temperature fails very quickly before the temperature stabilizes. While, in the tests with sufficient cooling, the temperature increases in the beginning of the test and stabilized after a few seconds. On the other hand, the temperature of the piezoelectric converter and the horn also increases which affects the displacement amplitude and stresses. So, these components are also cooled down using compressed air to prevent negative effects on the fatigue life of the specimen.

The generator used in the test setup is a Rinco Ultrasonics AGM20-1000P-230-B2 with maximum output power of 1 kW. It transmits an electrical sinusoidal signal with a predefined frequency of 20 kHz to the piezoelectric transducer. Then, the electrical signal is converted into mechanical vibrations through the transducer. The booster is selected to increase the amplitude of the mechanical vibrations delivered by the transducer with the ratio of 1:3. It is also used for clamping the whole system. After the booster, the horn is mounted to the system which can further amplify or de-amplify the vibrations. It is made out of aluminum by 2:1 ratio to reduce the displacements down to the representative values for a fatigue life up to 100 million cycles. The horn also performs as a connection between the specimen and the booster.

Ultrasonic fatigue tests can be performed using two different methods. The first approach is setting the generator power as a constant value and obtaining measurements as such. While being conceptually straightforward, the stress range may vary over the course of a test which is challenging from the perspective of test analysis. The second approach is to constantly control the displacement range at the free end of the specimen (which is linked to the stress range in the specimen) and change the power accordingly, using feedback electronics [20]. The procedure discussed in this paper is based on the first method and evaluates the variability of stress range as the test proceeds.

A schematic of the testing equipment is illustrated in Fig. 1. An Optris CTlaser LT-CF2 pyrometer is used for temperature measurement in the mid-section of the specimen, where the temperature is maximum. Moreover, a Keyence LK-H008W laser is used to measure the displacement amplitude at the free end of the specimen where the maximum displacement occurs. The sensors are connected to an NI-9223 data acquisition which obtains the data at a sampling frequency of 250 kHz and transfers it to a computer.

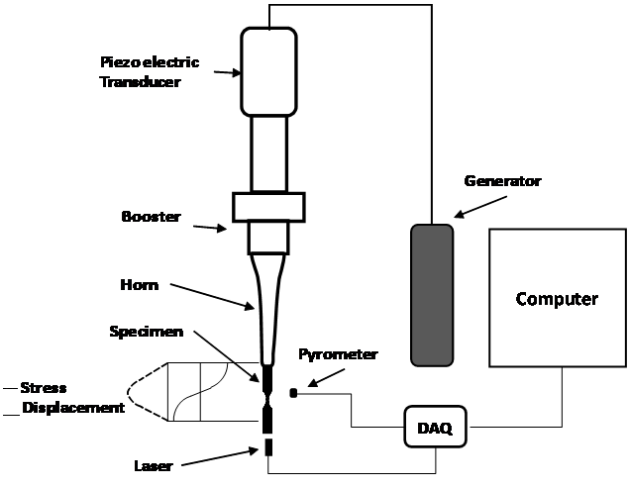

Fig. 1 Schematic of the ultrasonic fatigue testing set-up

III. Material and Design of Test Specimens

The material used in this experiment is a grey cast iron EN-GJL-250 with ferritic-pearlitic structure. Cast irons are distinguished from each other by the form of their graphite inclusions (or other carbon rich phases) [21]. Grey cast irons are often used for complex shaped components where tensile strength is not a concern, and damping properties are desirable (such as machine housings). They contain graphite flakes and are believed to have a fatigue limit equivalent to 25-30% of the ultimate tensile strength, but this approximation does not take into account the complex microstructure of the material [22]. Therefore, fatigue tests are required to define the actual values of fatigue strength.

As Bathias et al. [23] states crack initiation in cast alloys beyond 10^7 cycles is mainly due to the presence of porosities. Microporosities are usually the main cause of crack initiation in the powder metallurgy alloys.

The test specimens were designed to have the resonance

frequency of 20 kHz in their first vibration mode [1], [13], [24], corresponding to the frequency of the piezoelectric transducer.

Initially, the specimen geometry was designed analytically (making use of approximate relations). Then it was numerically tuned by means of finite element analysis to achieve a resonance frequency of 20 kHz.

The analytical solution for designing the specimen is given for specimens having a hyperbolic cosine shaped transition towards the reduced section. However, for convenience of manufacturing, the reduction in cross section is achieved by a circular arc transition. According to Bathias et al. [1], this is a good approximation, since the two curved shapes have a maximum geometrical difference of only 1.8%.

To design a round specimen with reduced cross section for ultrasonic fatigue testing, the following parameters need to be defined: diameter of the reduced section, *d*, diameter of the cylindrical part, *D*, and either the gauge length, *l*, or the radius, *r* (see Fig. 2). Given *d* and *D*, *r* and *l* are geometrically related. The diameter *D* is defined based on the material size (possibility of withdrawing the specimen out of the material), which according to [25], is usually between 10 to 15 mm. The gauge length *l*, or radius *r*, is determined given the desired stresses in the mid-section and the power of the ultrasonic machine. The larger the radius r or length l is, the smoother the stresses are distributed [25].

The maximum stress amplitude that occurs in the mid cross section is correlated with the specimen's deformation behavior based on (1) [1].

$$\sigma_a = A_0.E_d.\beta.\cos(\frac{\omega.L}{C}).\cosh(bl).(\frac{1}{\sinh(\beta l)}) \quad (1)$$

where:

$$\omega = 2\pi\upsilon \qquad C = \sqrt{\frac{E_d}{\rho}}$$

$$b = \frac{1}{l}\cosh^{-1}(\frac{D}{d}) \quad \beta = \sqrt{b^2 - (\frac{\omega}{C})2}$$

The length of the cylindrical part (the resonance length) is calculated through (2).

$$L = \frac{C}{\omega}\tan^{-1}[\frac{C}{\omega}(\beta.\coth(\beta.l) - b.\tanh(b.l)] \quad (2)$$

A_0 is the displacement amplitude at the free end of the specimen (measured by means of a laser sensor), E_d is the dynamic Young's modulus, υ is frequency, and ρ is density.

The specimens are connected directly to the horn using a threaded transition.

The dimensions of the specimens used for this work are presented in Table I.

To define the dynamic Young's modulus a solid bar with the diameter of 10 mm with the initial length of L_1, using static Young's modulus should be designed how it satisfies (3). The purpose is making this solid bar resonate in the frequency of 20 kHz and obtaining the dynamic Young's modulus through it. So, if the resonating frequency of the specimen with the initial length is lower than the required frequency, the specimen will be cut in length until acquiring the frequency of the purpose. Afterward, having the solid bar's final length, the dynamic Young's modulus is calculated through (3) [24].

$$L_1 = \frac{1}{2\upsilon}\sqrt{\frac{E}{\rho}} \quad (3)$$

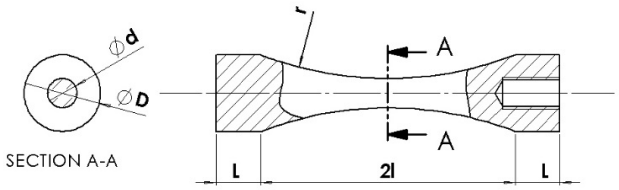

Fig. 2 Ultrasonic fatigue testing specimen

TABLE I
SPECIMEN DIMENSIONS IN MM

d	D	r	l	L
4.6	12.0	56	20	7

IV. EXPERIMENTAL PROCEDURE

In the ultra-high cycle loading region, surface finishing can affect the fatigue strength of the materials. According to [26], surface roughness is a source of stress concentration and leads to a shorter fatigue lifetime. In order to obtain similar surface roughness and residual stress for all specimens in addition to decreasing the scatter in the results [1], [27], the specimens are polished to have approximately the same roughness using the following procedure.

The specimens are polished in the reduced section prior to the test using sand paper with a sequence of 240, 400, and 1200 grit sizes until an R_a-value of 0.4-0.5 μm is obtained.

The free end of the specimens is also polished until no scratches are observed anymore to remove a source of scatter on the measured displacement at the bottom of the specimen.

The pyrometer was focused at the mid-section of the specimen, where the temperature is maximum, at a specific distance from the specimen. The laser sensor was focused at the bottom of the specimen and adjusted in the visible range of the sensor. Two sources of compressed air oriented towards the specimen, one source on the piezoelectric transducer and one source on the horn, were used for cooling the system during the test.

The tests were performed at ambient temperature by setting a constant generator power. Since the specimen's temperature stabilizes after a very short time up to 60°C and 70°C, an acceptable temperature increase for the investigated material, the tests were performed continuously until fracture occurred. Tests that did not fail after 10^8 cycles were considered as runouts and stopped without fracture.

An in-house made LabVIEW program was used to treat,

visualize, and collect the test data. The data were sampled at the frequency of 250 kHz. In most situations, every 3s, 200 samples were read. Afterwards, an in-house made MATLAB program was used for post processing the obtained data.

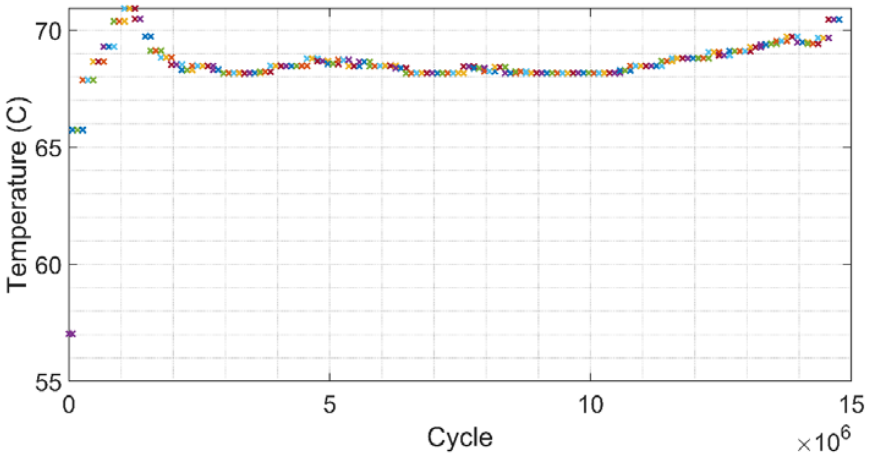

Fig. 3 Temperature evolution during the ultrasonic fatigue test

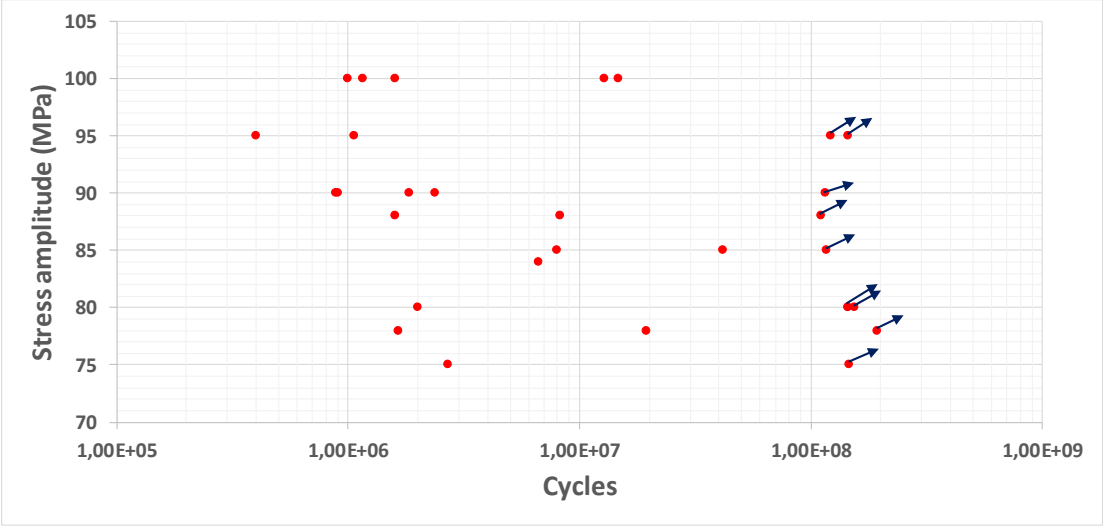

Fig. 4 The stress-life plot of the EN-GJL-250 specimens obtained by ultrasonic fatigue testing at 20 kHz

V. Results

Temperature variations during one of the fatigue tests are illustrated in Fig. 3. The test is performed by applying constant stress of 100 MPa through adjustment of the generator power at a constant value. As it shows, the temperature increases rapidly at the beginning of the test and it is followed by a stabilization. The initial increase is due to the mechanical energy dissipation in the tested specimen. The balance between the mechanical energy dissipation into heat, energy loss by convection and radiation at the surface and conduction in the specimen lead to the temperature stabilization.

Prior to final fracture, the specimen temperature increases rapidly again. That is an indication of crack propagation, which is confirmed to consume a minor part of the entire specimen lifetime.

The stress life results of the fatigue tests on the grey cast iron EN-GJL-250 is presented in Fig. 4 in a semi-log plot. The arrows indicate the runout tests (beyond 10^8 cycles).

A large scatter of the test results is observed. Variation of the size and distribution of internal defects could cause the scatter among the results. Moreover, since the fatigue life is dominated by crack initiation in ultra-high cycle regime slight differences in microstructure could be another reason of the scatter among the results.

The fractured surface of some of the failed specimens were analyzed by scanning electron microscopy (SEM). SEM results indicated occurrence of the fatigue crack initiation of all GG25 specimens inside the material from an internal defect as it is clear in Fig. 5.

Here a porosity is the main reason of crack initiation.

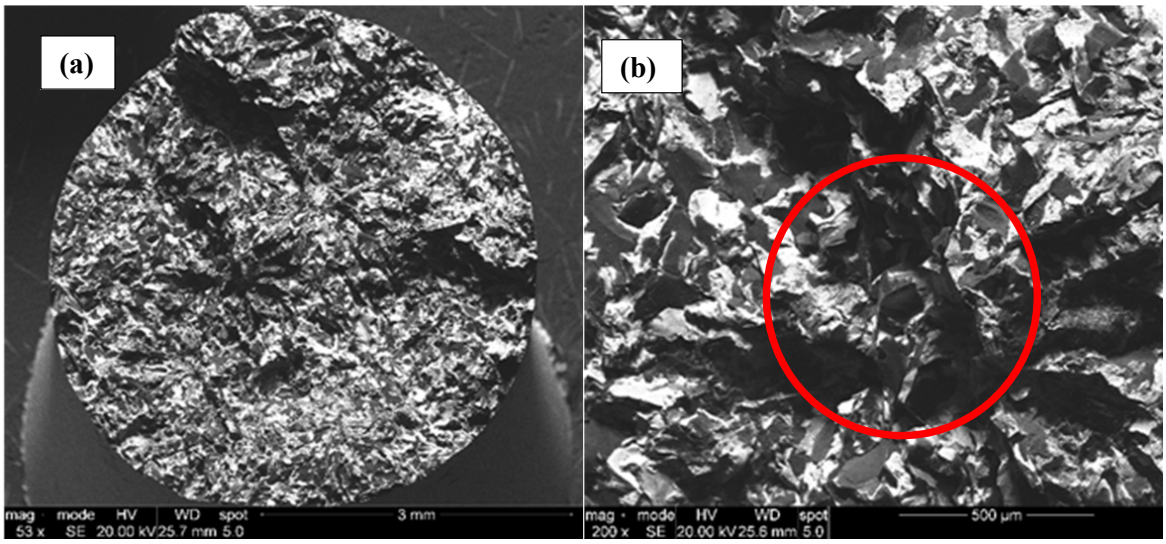

Fig. 5 Fractography of the fractured surface of a EN-GJL-250 specimen using SEM. (a) the fractured surface, (b) the crack initiation area

ACKNOWLEDGMENT

The authors gratefully acknowledge the financial support of Vlaio, and professor Roumen Petrov for his support with SEM fractography.

REFERENCES

[1] C. Bathias and P. C. Paris, *Gigacycle fatigue in mechanical practice* vol. 185: CRC Press, 2004, pp. 19-119.
[2] "Eurocode 3- Design of steel structures - Part 1-9_ EN 1993-1-9," ed, 2005.
[3] " Eurocode 9. Design of aluminium structures. Structures susceptible to fatigue, Part2," ed, 1999-2:2000.
[4] C. Bathias, "There is no infinite fatigue life in metallic materials," *Fatigue and fracture of engineering materials and structures,* vol. 22, pp. 559-566, 1999.
[5] C. Sonsino, "Course of SN-curves especially in the high-cycle fatigue regime with regard to component design and safety," *International Journal of Fatigue,* vol. 29, pp. 2246-2258, 2007.
[6] C. Bathias, "Influence of the metallurgical instability on the gigacycle fatigue regime," International Journal of Fatigue, vol. 32, pp. 535-540, 2010.
[7] C. Wang, D. Wagner, Q. Wang, and C. Bathias, "Gigacycle fatigue initiation mechanism in Armco iron," *International Journal of Fatigue,* vol. 45, pp. 91-97, 2012.
[8] H. Mughrabi, "On 'multi-stage'fatigue life diagrams and the relevant life-controlling mechanisms in ultrahigh-cycle fatigue," *Fatigue & Fracture of Engineering Materials & Structures,* vol. 25, pp. 755-764, 2002.
[9] C. Wang, J. Petit, Z. Huang, and D. Wagner, "Investigation of crack initiation mechanisms responsible for the fish eye formation in the Very High Cycle Fatigue regime," International Journal of Fatigue, vol. 119, pp. 320-329, 2019.
[10] Y. Hong and C. Sun, "The nature and the mechanism of crack initiation and early growth for very-high-cycle fatigue of metallic materials–An overview," Theoretical and Applied Fracture Mechanics, vol. 92, pp. 331-350, 2017.
[11] W. P. Mason, "Piezoelectronic Crystal and Their Application in Ultrasonics," *Van Nostrand,* p. 161, 1950.
[12] Y. Lage, M. Freitas, L. Reis, A. Ribeiro, and D. Montalvão, "Instumentation of Ultrasonic High-Frequency Machine to Estimate Applied Stress in Middle Section of Specimen," in Procs of 15th International Conference on Experimental Mechanics, 2012.
[13] Y. Lage, A. Ribeiro, D. Montalvão, L. Reis, and M. Freitas, "Automation in strain and temperature control on VHCF with an ultrasonic testing facility," in Application of Automation Technology in Fatigue and Fracture Testing and Analysis, ed: ASTM International, 2014.
[14] H. Mayer, "Ultrasonic torsion and tension–compression fatigue testing: Measuring principles and investigations on 2024-T351 aluminium alloy," International Journal of Fatigue, vol. 28, pp. 1446-1455, 2006.
[15] C. Bathias, "Piezoelectric fatigue testing machines and devices," International Journal of Fatigue, vol. 28, pp. 1438-1445, 2006.
[16] V. Anes, D. Montalvao, A. Ribeiro, M. Freitas, and M. Fonte, "Design and instrumentation of an ultrasonic fatigue testing machine," 2011.
[17] D. Wagner, F. J. Cavalieri, C. Bathias, and N. Ranc, "Ultrasonic fatigue tests at high temperature on an austenitic steel," Propulsion and Power Research, vol. 1, pp. 29-35, 2012.
[18] L. Xu, Q. Wang, and M. Zhou, "Micro-crack initiation and propagation in a high strength aluminum alloy during very high cycle fatigue," Materials Science and Engineering: A, vol. 715, pp. 404-413, 2018.
[19] S. Stanzl-Tschegg and H. Mayer, "Fatigue and fatigue crack growth of aluminium alloys at very high numbers of cycles," International Journal of Fatigue, vol. 23, pp. 231-237, 2001.
[20] Y. Lage, M. Freitas, D. Montalvao, A. Ribeiro, and L. Reis, "Ultrasonic fatigue analysis on steel specimen with temperature control: evaluation of variable temperature effect," 2012.
[21] A. Gulyaev, "Physical Metallurgy (in Russian), Metallurgiya, Moscow (1977)," Google Scholar, p. 647.
[22] T. Willidal, W. Bauer, and P. Schumacher, "Stress/strain behaviour and fatigue limit of grey cast iron," Materials Science and Engineering: A, vol. 413, pp. 578-582, 2005.
[23] C. Bathias and A. Pineau, Fatigue of materials and structures: Wiley Online Library, 2010.
[24] F. Cavalieri, C. Bathias, N. Ranc, A. Cardona, and J. Risso, "Ultrasonic fatigue analysis on an austenitic steel at high temperature," Mecánica Computacional, vol. 27, pp. 1205-1224, 2008.
[25] L. Trško, F. Nový, O. Bokůvka, and M. Jambor, "Ultrasonic Fatigue Testing in the Tension-Compression Mode," Journal of visualized experiments: JoVE, 2018.
[26] I. Marines, G. Dominguez, G. Baudry, J.-F. Vittori, S. Rathery, J.-P. Doucet, et al., "Ultrasonic fatigue tests on bearing steel AISI-SAE 52100 at frequency of 20 and 30 kHz," International Journal of Fatigue, vol. 25, pp. 1037-1046, 2003.
[27] N. Schneider, J. Bödecker, C. Berger, and M. Oechsner, "Frequency effect and influence of testing technique on the fatigue behaviour of quenched and tempered steel and aluminium alloy," International Journal of Fatigue, vol. 93, pp. 224-231, 2016.